

# Anomalous Fluctuations of Extremes in Many-Particle Diffusion

Jacob B Hass, Aileen N Carroll-Godfrey, and Eric I Corwin  
*Department of Physics and Materials Science Institute,  
University of Oregon, Eugene, Oregon 97403, USA.*

Ivan Z Corwin  
*Department of Mathematics, Columbia University, New York, New York 10027, USA.*  
(Dated: May 6, 2022)

In many-particle diffusions, particles that move the furthest and fastest can play an outsized role in physical phenomena. A theoretical understanding of the behavior of such extreme particles is nascent. A classical model, in the spirit of Einstein’s treatment of single-particle diffusion, has each particle taking independent homogeneous random walks. This, however, neglects the fact that all particles diffuse in a common and often inhomogeneous environment that can affect their motion. A more sophisticated model treats this common environment as a space-time random biasing field which influences each particle’s independent motion. While the bulk (or typical particle) behavior of these two models has been found to match to high degree, recent theoretical work of Barraquand, Corwin and Le Doussal on a one-dimensional exactly solvable version of this random environment model suggests that the extreme behavior is quite different between the two models. We transform these asymptotic (in system size and time) results into physically applicable predictions. Using high precision numerical simulations we reconcile different asymptotic phases in a manner that matches numerics down to realistic system sizes, amenable to experimental confirmation. We characterize the behavior of extreme diffusion in the random environment model by the presence of a new phase with anomalous fluctuations related to the Kardar-Parisi-Zhang universality class and equation.

*Introduction*— Our world is fueled by outliers. Information in signals is carried by the leading edge [1–8]. A viral or bacterial infection is spread by the first few pathogens to enter a host and the first host to enter a new region [9, 10]. A species is evolved by the fittest mutations [11–13]. Scientific revolution is sparked by the first new idea. In all of these contexts the precipitating action is driven by the extremes among a great number of agents (varying from  $N \sim 10^2$  to  $N \sim 10^{60}$  depending on the context) evolving in a complex but shared environment. How does the nature of the shared environment affect these outlier behaviors? Conversely, can we infer the nature of the shared environment from the behavior of these outliers? Despite their obvious importance, these overarching questions are still unanswered.

The classical model for many-particle diffusion as independent homogeneous random walks provides an easily calculable solution, but entirely neglects the effects of the shared and likely inhomogeneous environment. This model is the basis for Einstein’s diffusion coefficient [14–16], which succinctly describes the behavior of typical particles in a many-particle diffusion. A more sophisticated model treats the shared environment as a space-time random biasing field with short-range space-time correlations. Each particle thus articulates independent random walks subject to forcing by the common biasing field. While this refined model does not impact typical particle diffusion behavior [17], it drastically impacts the behavior of extreme particles. In this work, we provide predictions for the behavior of extreme particles moving in a random and inhomogeneous environment. We find that the variance in the position of the extreme particle is a robust and sensitive measurement of the nature

of the environment and show how this variance can be understood as the sum of two contributions: the randomness present in the environment, and the sampling of random walks in that environment. We show that by subtracting out the variance due to sampling we can produce direct measurements of the environment, inaccessible from measurements of the motion of a typical particle or of the bulk. This residual environmental variance is characterized by a novel power law that we demonstrate holds even when the number of particles is very small.

*Background*— Building on observations by Brown [18, 19] from 1827, Einstein [14–16] (along with Langevin [20], Sutherland [21, 22] and Smoluchowski [23, 24]) proposed a theory of diffusion based on modeling particles by independent random walks with variance controlled by a diffusion coefficient intrinsic to the particle/environment pair. Soon after, Perrin experimentally verified Einstein’s statistical predictions [25, 26].

Probing the effectiveness and limitations of Einstein’s diffusion model has remained a challenge. On short time scales, particle motion is ballistic, dominated by inertia [27, 28]. Many physically relevant situations require the addition of new concepts to accurately model them. Certain diffusive processes are better modeled by Levy flights [29] or other types of anomalous diffusions [30, 31] instead of simple random walks. Other work has focused on particles able to inject energy into the environment, leading to the notion of active materials [32, 33]. Further, in environments which are slowly mixing, Einstein’s theory may also break down due to the presence of quenched disorder [29, 34]. Unlike the above deviations from the classical model, our approach is intended to describe generic many-particle diffusions.

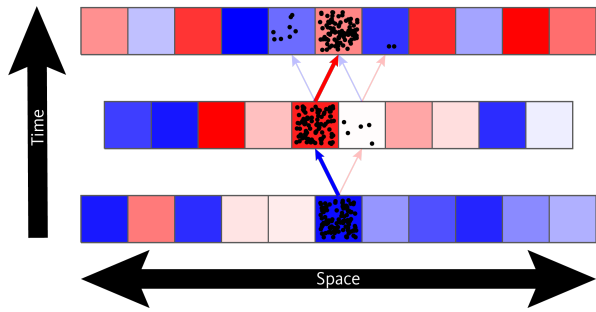


FIG. 1. The spatial locations (horizontal axis) of  $N = 10^2$  Beta-RWRE particles over time (vertical axis). The color indicates the bias (red is right biased and blue is left biased) and is chosen independently at each space-time box. The location of particles within each box is chosen for ease of visualization.

The random walk in random environment (RWRE) model we consider here goes back to [35, 36] (see also [37–40]) and comes in two types – long-range [30, 41–45] and short-range [46–52] temporally correlated environments. We focus here on the latter type. In this context typical RWRE particles behave like Brownian motion, matching the behavior from Einstein’s model [53, 54].

The motion of atypical particles is controlled by large deviations of the RWRE’s transition probability. The study of RWRE large deviations was initiated in [55]. Barraquand and Corwin [56] discovered the first exactly solvable RWRE model – the Beta RWRE discussed extensively below – and uncovered a remarkable connection between its large deviations and the Kardar-Parisi-Zhang (KPZ) universality class’s [57, 58] Tracy-Widom GUE distribution [59]. This connection obtains for times comparable to  $\log(N)$ . This model was further studied in [60] which recognized that a phase transition should occur in the  $(\log(N))^2$  time frame. This was brought into focus in [61] which discovered that in this scale the Tracy-Widom GUE distribution is replaced by that of the KPZ equation [62–66] confirming some predictions of [60]. See [67–73] for further developments. The occurrence of the KPZ equation / universality class in the large deviations for RWREs was unexpected and is useful as the statistics associated to these objects are well studied theoretically and numerically. Moreover, there is evidence that both the equation and universality class have wide domains of attraction [74–76], suggesting that results shown for the solvable Beta RWRE model should apply more broadly.

*Models for diffusion*— Though physical diffusion is continuous in time and (typically) occurs in three-dimensional space, here we work with discrete models in one spatial dimension. Discretization is common for numerical simulations and working in one dimension skirts anisotropy issues arising from the choice of lattice in higher dimensions. This is also the setting for the exactly solvable RWRE [56], though a continuous limit of that model exists [69]. In real diffusion in a common environment, there will be length and time scales on which

the environment decorrelates. Our discrete model can be thought of as coarse-graining the environment in space and time onto a lattice. Our model does not directly address the higher order interactions among particles and between particles and the environment. We expect these higher order effects will be less present in the behavior of extreme particles since the local density of particles around the extremes is necessarily low and thus interactions play a weaker role. We also expect long-time and large-scale behavior of discrete and continuous models should not greatly differ. Additionally, there are physical settings where particles take discrete states (such as in phylogenetic evolution over time [77, 78] where the short length and time behavior may be physically relevant) or evolve in quasi-one-dimensional spaces (such as in diffusion through thin capillary tubes [79, 80]).

We study the *Beta RWRE* introduced in [56] (see Fig. 1). We model the environment by a collection  $\mathbf{B} = \{B(x, t) : x \in \mathbb{Z}, t \in \mathbb{Z}_{\geq 0}\}$  of independent identically distributed random variables all drawn from the uniform distribution on the interval  $[0, 1]$ . At time  $t = 0$  we start with  $N$  particles (i.e. random walkers) all at site 0. Given an instance of the environment  $\mathbf{B}$  the particles proceed in the following manner. Each particle at location  $x$  at time  $t$  (starting with  $t = 0$  and proceeding recursively to larger  $t = 1, 2, \dots$ ) independently flip the same weighted coin which has probability  $B(x, t)$  of heads (moving the particle to site  $x + 1$  at time  $t + 1$ ) and  $1 - B(x, t)$  of tails (moving to  $x - 1$  instead). Consequently, if there are  $N(x, t)$  particles at site  $x$  at time  $t$ , then the number that move to the right (to site  $x + 1$ ) is binomially distributed with  $N(x, t)$  samples and success probability  $B(x, t)$  (the remainder move left to site  $x - 1$ ). Thus, while particles do not interact with each other, those at the same place and time are all influenced by the common environment.

This model is exactly solvable when the environment biases  $B(x, t)$  are distributed according to the Beta distribution  $Beta(\alpha, \beta)$  [56]. For simplicity, we focus here on the special case  $\alpha = \beta = 1$  corresponding to the uniform distribution. The classical simple symmetric random walk (SSRW) model arises in the limit  $\alpha = \beta \rightarrow \infty$  where all  $B(x, t) \equiv 1/2$  and hence all coin flips are fair and the environment is deterministic.

We will be concerned with the behavior of the right-most particle at time  $t$ . We denote this by  $\text{Max}_t^N$ , with  $N$  representing the number of particles in the system in total. Two types of randomness affect  $\text{Max}_t^N$ , that of the environment and that of sampling the random walks in that environment. The effect of the environment is via the transition probability  $p_{\mathbf{B}}(x, t)$ , defined as the probability that a single random walker initially at 0 at time 0 will end up at  $x$  at time  $t$  for a given environment  $\mathbf{B}$ . This satisfies the recursion relationship (i.e., the Kolmogorov backward equation, or master equation),

$$p_{\mathbf{B}}(x, t) = p_{\mathbf{B}}(x - 1, t - 1)B(x - 1, t - 1) + p_{\mathbf{B}}(x + 1, t - 1)(1 - B(x + 1, t - 1)) \quad (1)$$

with initial condition  $p_{\mathbf{B}}(0, 0) = 1$  and  $p_{\mathbf{B}}(x \neq 0, 0) = 0$ . Since each random walker is independent, conditional on the environment, the distribution of the ensemble of  $N$  walks is entirely determined by  $p_{\mathbf{B}}(x, t)$ . For instance, given the environment  $\mathbf{B}$ , the probability that a single random walker ends up at or above  $x$  at time  $t$  is given by the tail probability,  $P_{\mathbf{B}}(x, t) = \sum_{y \geq x} p_{\mathbf{B}}(y, t)$ . From this and the independence of random walkers, conditional on the environment, it follows that

$$\text{Prob}_{\mathbf{B}}(\text{Max}_t^N \leq x) = (1 - P_{\mathbf{B}}(x, t))^N, \quad (2)$$

where the left-hand side is the probability, given the environment  $\mathbf{B}$ , that  $\text{Max}_t^N \leq x$ . For the SSRW where  $B(x, t) \equiv 1/2$ , we use the same notation  $p(x, t)$  and  $P(x, t)$ , dropping the  $\mathbf{B}$  subscript. We note that  $p(x, t)$  is now given by a binomial coefficient.

We are interested in how  $\text{Max}_t^N$  varies upon sampling a new environment and random walkers therein. Eq. (2) suggests that a good proxy for  $\text{Max}_t^N$  will be the location  $\text{Env}_t^N$  of the  $1/N$ -quantile of the distribution function  $P_{\mathbf{B}}(x, t)$ , i.e.,  $\text{Env}_t^N$  equals the maximal  $x$  such that  $P_{\mathbf{B}}(x, t) > 1/N$ . Notice that  $\text{Env}_t^N$  only accounts for the variation due to the environment. The variation due to sampling in that environment will be denoted by  $\text{Sam}_t^N$  and defined by the equality  $\text{Max}_t^N = \text{Env}_t^N + \text{Sam}_t^N$ . We will use the notation  $\text{Mean}(\bullet)$  and  $\text{Var}(\bullet)$  for the mean and variance of a quantity  $\bullet$  (e.g.  $\text{Max}_t^N, \text{Env}_t^N, \text{Sam}_t^N$ ) averaged over both the environment and the sampling of random walkers in that environment.

*Numerical Methods*— We numerically simulate our models for system sizes varying from  $N = 10^2$  to  $N = 10^{300}$ . We evolve the system for times from  $t = 0$  to  $t = 5000 \log(N)$ . As explained below,  $\log(N)$  and  $(\log(N))^2$  set key timescales and our range of times ensure that for all choices of  $N$ , our numerics sweep out these scales. We simulate such large systems by utilizing the full range of quadruple-precision floating point numbers and making approximations to the binomial distribution when dealing with sizes beyond our precision limits, as described in [81]. The rightmost particle at each time represents a sample of  $\text{Max}_t^N$ . By repeatedly sampling new environments along with random walks therein we numerically measure the value of  $\text{Var}(\text{Max}_t^N)$ . To distinguish from the true value we denote this numerically measured variance by  $\text{Var}^{\text{num}}(\text{Max}_t^N)$  and plot it in Fig. 2. In like fashion, we measure  $\text{Var}^{\text{num}}(\text{Env}_t^N)$  for each sampled environment by using Eq. 1 to compute  $p_{\mathbf{B}}(x, t)$ . Fig. 3 shows  $\text{Var}^{\text{num}}(\text{Env}_t^N)$  as a function of time (see [81] for  $\text{Mean}^{\text{num}}(\text{Max}_t^N)$  and  $\text{Mean}^{\text{num}}(\text{Env}_t^N)$ ).

*Asymptotic Theory Results*— We describe asymptotic results on the behavior of  $\text{Max}_t^N, \text{Env}_t^N$  and  $\text{Sam}_t^N$  as both  $N$  and  $t$  tend to infinity in different limits. Interpolating back from these asymptotics we provide theoretical formulas for finite  $N$  and  $t$ . We use the notation  $\text{Var}^{\text{asy}}(\bullet)$  to denote the asymptotic theoretical formula for the vari-

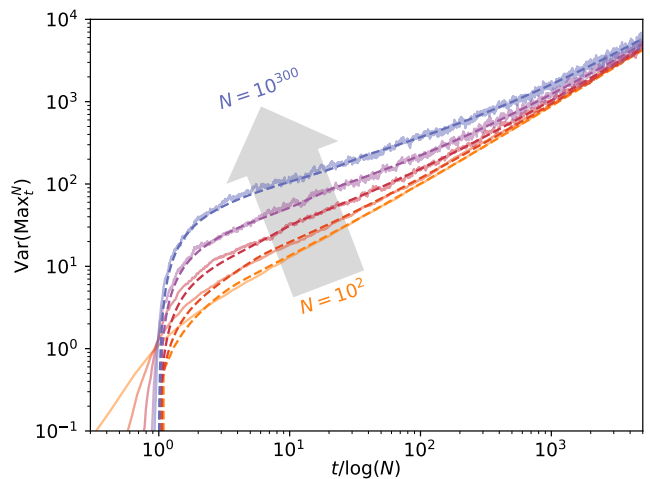


FIG. 2. The variance of the maximum particle for  $N = 10^2, 10^7, 10^{24}, 10^{85}$  and  $10^{300}$  for 10000, 5000, 1500, 500 and 500 instantiations of the environment, respectively. Solid lines are  $\text{Var}^{\text{num}}(\text{Max}_t^N)$  and dashed lines are  $\text{Var}^{\text{asy}}(\text{Max}_t^N)$ .

ance of  $\bullet$ . The asymptotic theory for the SSRW is classical, following from Stirling's formula (or more generally large deviation theory). Asymptotic results for the RWRE rely on more sophisticated tools coming from the field of quantum integrable systems [56, 61, 73] and are derived first for  $\text{Env}_t^N$  and then for  $\text{Max}_t^N$  and  $\text{Sam}_t^N$ .

**SSRW  $\text{Max}_t^N$ :** For  $t/\log(N)$  bounded below  $(\log 2)^{-1}$ , we have  $N \gg 2^t$  and hence there are so many particles that with very high probability the random walks saturate every reachable site in the lattice at time  $t$  and hence  $\text{Var}(\text{Max}_t^N) \approx 0$ . When  $t/\log(N) > (\log 2)^{-1}$ , the location of the maximal random walk at time  $t$  will likely occur at a position significantly below  $t$  and have non-trivial fluctuations which can be calculated by combining (2) with Stirling's formula for binomial coefficient asymptotics. Doing this in [81] we see that  $\text{Max}_t^N$  is asymptotically distributed as a Gumbel random variable with explicit mean and variance. In particular, for  $t \gg \log(N)$ ,  $\text{Var}^{\text{asy}}(\text{Max}_t^N) \approx \frac{\pi^2}{12} \frac{t}{\log(N)}$ .

**RWRE  $\text{Env}_t^N$ :** For  $t/\log(N) < 1$ ,  $\text{Var}(\text{Env}_t^N) \approx 0$ . To see this, note that  $P_{\mathbf{B}}(t, t) = B_{0,0} B_{1,1} \cdots B_{t-1,t-1}$ . Taking logarithms and applying the central limit theorem shows that  $\log(P_{\mathbf{B}}(t, t)) \approx -t + t^{1/2}G$  for  $G$  a standard Gaussian random variable. This implies that  $P_{\mathbf{B}}(t, t) \approx e^{-t}$  which is much larger than  $1/N$  for  $t/\log(N) < 1$ . This shows that the RWRE model stops saturating the lattice for  $t \approx \log(N)$  plus a Gaussian fluctuation of order  $(\log(N))^{1/2}$  which should be compared to the SSRW which stops saturating at a later time  $\log_2(N)$  but with order one fluctuations.

$\text{Var}(\text{Env}_t^N)$  displays two regimes of non-trivial asymptotic fluctuations that relate to the long-time and short-time scaling behavior of the KPZ equation. For  $t/\log(N)$  converging to a finite value exceeding 1, as derived in [81]

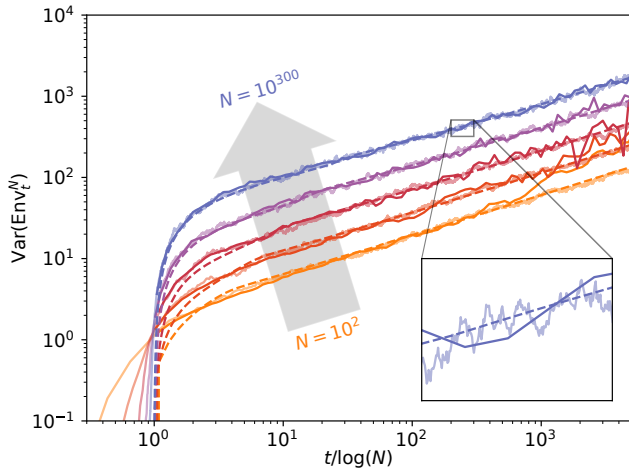


FIG. 3. Comparison for system sizes  $N = 10^2, 10^7, 10^{24}, 10^{85}$  and  $10^{300}$  between three methods to compute  $\text{Var}(\text{Env}_t^N)$ , the variance due to the random environment of the location of the  $1/N$ -quantile. The transparent solid line records the numerical measurement  $\text{Var}^{\text{num}}(\text{Env}_t^N)$  computed by sampling 500 instantiations of the environment. The dashed line records  $\text{Var}^{\text{asy}}(\text{Env}_t^N)$ . The darker solid line records  $\text{Var}^{\text{num}}(\text{Max}_t^N) - \text{Var}^{\text{asy}}(\text{Sam}_t^N)$ , the numerically observed variance of the maximum of  $N$  random walkers at time  $t$  minus the asymptotic formula for the variance of  $\text{Sam}_t^N$ . We divide each decade in time into 25 bins and take the arithmetic mean to smooth  $\text{Var}^{\text{num}}(\text{Max}_t^N) - \text{Var}^{\text{asy}}(\text{Sam}_t^N)$ . The three curves agree well, as shown in the zoomed-in inset.

$\text{Var}(\text{Env}_t^N)$  takes the asymptotic form [56],

$$\left(\frac{\log(N)}{t}\right)^{2/3} \sigma_\chi^2 \frac{2^{2/3} \left(1 - \frac{\log(N)}{t}\right)^{4/3}}{1 - \left(1 - \frac{\log(N)}{t}\right)^2}, \quad (3)$$

where  $\chi$  is Tracy-Widom GUE [59] distributed with variance  $\sigma_\chi^2 \approx 0.813$  [82]. If instead, the ratio of  $t/(\log(N))^2$  converges to a finite value, then, as derived in [81],  $\text{Var}(\text{Env}_t^N)$  takes the asymptotic form [61],

$$\frac{t}{2 \log(N)} \cdot \text{Var} \left( h \left( 0, \frac{4(\log(N))^2}{t} \right) \right), \quad (4)$$

where  $h(0, s)$  denotes the (random) height at 0 and time  $s$  of the *narrow wedge* solution to the KPZ equation.

Interpolating between these two regimes, and extrapolating past the  $(\log(N))^2$  regime (see also [73]) we find two power-laws,

$$\text{Var}^{\text{asy}}(\text{Env}_t^N) \approx \begin{cases} \sigma_\chi^2 \left(\frac{\log(N)}{2}\right)^{\frac{1}{3}} t^{\frac{1}{3}} & 1 \ll \frac{t}{\log(N)} \ll \log(N), \\ \frac{1}{2} \pi^{\frac{1}{2}} t^{\frac{1}{2}} & \frac{t}{\log(N)} \gg \log(N). \end{cases} \quad (5)$$

For finite  $N$  and  $t$  these regimes have a long and gentle crossover that we capture in the function  $\text{Var}^{\text{asy}}(\text{Env}_t^N)$  by stitching together (3) and (4) with an error function centered at  $(\log(N))^{3/2}$  of width  $(\log(N))^{4/3}$ .

**RWRE  $\text{Sam}_t^N$ :** We identify the additional contribution to the full extreme particle behavior,  $\text{Max}_t^N$ , from sampling the many-particle diffusion given an environment. In [81] we show that for  $t/\log(N)$  converging to a finite value exceeding 1, the sample fluctuation  $\text{Sam}_t^N$  is of Gumbel type with variance

$$\text{Var}^{\text{asy}}(\text{Sam}_t^N) = \frac{\pi^2}{6 \log(N)} \frac{\left(\frac{t}{\log(N)} - 1\right)^2}{2 \frac{t}{\log(N)} - 1} \approx \frac{\pi^2}{12} \frac{t}{\log(N)}. \quad (6)$$

The approximation is in the limit when  $t/\log(N) \gg 1$  and matches the asymptotic behavior of the variance in the classical SSRW model in which there is no environmental fluctuation.

**RWRE  $\text{Max}_t^N$ :** As demonstrated in [81], the sample fluctuation  $\text{Sam}_t^N$  is asymptotically independent of the environmental fluctuation  $\text{Env}_t^N$ , thus

$$\text{Var}(\text{Max}_t^N) \approx \text{Var}(\text{Env}_t^N) + \text{Var}(\text{Sam}_t^N). \quad (7)$$

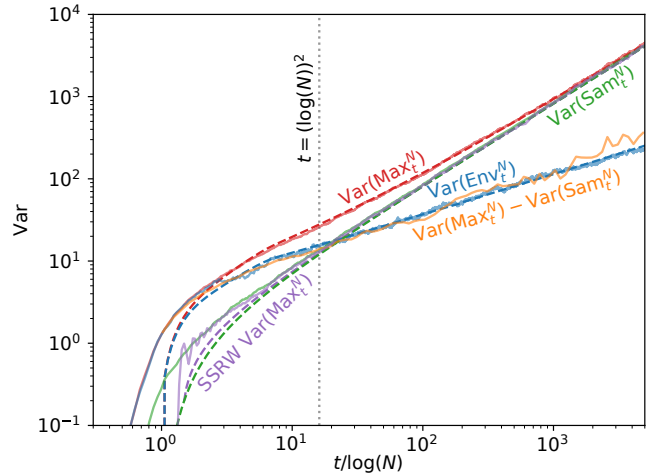


FIG. 4. For the  $N = 10^7$  RWRE model we plot the variance of the extreme particle  $\text{Var}(\text{Max}_t^N)$  (red), as well as the environmental contribution  $\text{Var}(\text{Env}_t^N)$  (blue), and sampling contribution  $\text{Var}(\text{Sam}_t^N)$  (green); for the  $N = 10^7$  SSRW model we plot the variance of the extreme particle  $\text{Var}(\text{Max}_t^N)$  (purple). The dashed lines are the asymptotic theoretical curves, i.e.  $\text{Var}^{\text{asy}}(\bullet)$ , corresponding to their color while the solid lines are the numerically measured curves, i.e.  $\text{Var}^{\text{num}}(\bullet)$ . The orange curve is  $\text{Var}^{\text{num}}(\text{Max}_t^N) - \text{Var}^{\text{asy}}(\text{Sam}_t^N)$  and closely matches the blue environmental variance curves. Again, we divide each decade in time into 25 bins and take the arithmetic mean to smooth  $\text{Var}^{\text{num}}(\text{Max}_t^N) - \text{Var}^{\text{asy}}(\text{Sam}_t^N)$ . The vertical dotted line indicates the regime crossover at  $t = (\log(N))^2$ .

*Comparison of Numerical and Theoretical Results*— Fig. 2 and 3 show that the asymptotic theoretical predictions (dashed lines) for  $\text{Var}(\text{Max}_t^N)$  and  $\text{Var}(\text{Env}_t^N)$  are in excellent agreement with the numerical measurements (solid lines). Fig. 3 further shows that when one subtracts the asymptotic variance  $\text{Var}^{\text{asy}}(\text{Sam}_t^N)$  from the

numerically measured  $\text{Var}^{\text{num}}(\text{Max}_t^N)$  we reliably recover  $\text{Var}(\text{Env}_t^N)$ , as expected from Eq. 7. Notably, while these results were derived for asymptotically large  $\log(N)$  and  $t$ , they hold nearly perfectly all the way down to  $N = 10^2$ . Fig. 3 reveals that while we readily see the long-time  $t^{1/2}$  power-law for  $\text{Var}(\text{Env}_t^N)$  from Eq. 5, the other  $t^{1/3}$  power-law is elusive. Although the full characterization of the short-time regime is in excellent agreement with the numerical results, the  $t^{1/3}$  power-law is difficult to capture since the transitional window of  $\log(N)$  to  $(\log(N))^2$  is too narrow for realistic sizes of  $N$ . Fig. 4 shows the tight matching of the asymptotic theory curves and numerically measured values for the variance of  $\text{Max}_t^N$ ,  $\text{Env}_t^N$  and  $\text{Sam}_t^N$  for a given value of  $N = 10^7$ . Notice that in this figure and the previous ones, for  $t \approx \log(N)$  the asymptotic theory and numerical values for the variance of  $\text{Sam}_t^N$  do not fit quite as well as for large  $t$ . This is likely a result of finite-size effects and quickly goes away at large values of  $t$  which are our main interest anyway.

**Conclusion**— We expect that much of the picture presented here will persist beyond the discrete and solvable model setting and be observable in experiments. The behavior for  $t$  on the order of  $\log(N)$  should be non-universal and depend in a non-trivial and difficult to characterize manner on the nature of the environment and diffusion therein. On the other hand, for  $t$  of any order exceeding  $\log(N)$ , we anticipate that the scaling exponents relating the variances of  $\text{Env}_t^N$ ,  $\text{Sam}_t^N$  and  $\text{Max}_t^N$  to  $t$  and  $\log(N)$  will be universal, as will the addition law (7). The coefficient for the environment variance in (5) should be non-universal and hold within it all of the accessible information about the correlation structure of the environment – we call this the *extreme diffusion coefficient*. Generalizing the model further to consider the Beta RWRE with parameters  $\alpha \neq \beta \neq 1$  or more general

distributions than Beta will provide a testing-ground for this universality. Considering higher dimensions as in [60] may lead to more discoveries that better model physical systems with spatial correlations. We have focused here primarily on the variance (the mean is also addressed in [81]). A study of higher order cumulants may reveal other ways to probe the hidden environment, though may be harder to observe numerically or experimentally.

In physical systems it is impossible to directly measure the environmental variance. However, an indirect measurement can be performed via the approach presented here by using  $\text{Var}(\text{Env}_t^N) \approx \text{Var}(\text{Max}_t^N) - \text{Var}(\text{Sam}_t^N)$ . The sample variance  $\text{Var}(\text{Sam}_t^N)$  is now computed using  $\text{Var}(\text{Sam}_t^N) = \frac{\pi^2 D}{6} \frac{t}{\log(N)}$  where  $D$  is the Einstein diffusion coefficient. By measuring the environmental variance and extreme diffusion coefficient we will gain a new microscope through which to probe the hidden nature of the underlying environment in which the diffusion occurs. Our work should serve as a guide in the development and analysis of novel experimental measurements of the extreme behavior of many-particle diffusion.

**Acknowledgements**— We thank G. Barraquand and P. Le Doussal for discussions and S. Prolhac for providing numerics for  $\text{Var}(h(0, s))$ . This work was funded under the W.M. Keck Foundation Science and Engineering grant on “Extreme Diffusion”. I.C. also wishes to acknowledge ongoing support from the NSF through DMS:1811143 and DMS:1937254, the Simon Foundation through a Simons Fellowship in Mathematics (Grant No. 817655), and the Packard Foundation Fellowship for Science and Engineering. Much of this work was performed while I.C. held a Miller Visiting Professorship from the Miller Institute for Basic Research in Science, and while in residence at the Mathematical Sciences Research Institute in Berkeley, California (NSF Grant No. 1440140). E. C. wishes to acknowledge ongoing support from the Simons Foundation for the collaboration Cracking the Glass Problem via award 454939.

- 
- [1] Michael J. Saxton and Ken Jacobson. Single-particle tracking: Applications to membrane dynamics. *Annual Review of Biophysics and Biomolecular Structure*, 26:373–399, 1997.
- [2] Philip A. Pinto and Ronald G. Eastman. The Physics of Type Ia Supernova Light Curves. II. Opacity and Diffusion. *The Astrophysical Journal*, 530(2):757–776, February 2000.
- [3] Felix Höfling and Thomas Franosch. Anomalous transport in the crowded world of biological cells. *Reports on Progress in Physics*, 76(4), 2013.
- [4] Surya K. Ghosh, Andrey G. Cherstvy, and Ralf Metzler. Non-universal tracer diffusion in crowded media of non-inert obstacles. *Physical Chemistry Chemical Physics*, 17(3):1847–1858, January 2015.
- [5] Carlo Manzo and Maria F. Garcia-Parajo. A review of progress in single particle tracking: From methods to biological insights. *Reports on Progress in Physics*, 78(12), 2015.
- [6] Srividya Iyer-Biswas and Anton Zilman. First Passage processes in cellular biology. *Advances in Chemical Physics*, 160:261–306, March 2015.
- [7] R. Metzler, J.-H. Jeon, and A. G. Cherstvy. Non-Brownian diffusion in lipid membranes: Experiments and simulations. *Biochimica Et Biophysica Acta*, 1858(10):2451–2467, October 2016.
- [8] Hao Shen, Lawrence J. Tauzin, Rashad Baiyasi, Wenxiao Wang, Nicholas Moringo, Bo Shuang, and Christy F. Landes. Single Particle Tracking: From Theory to Biological Applications. *Chemical Reviews*, 117(11):7331–7376, June 2017.
- [9] L. Hufnagel, D. Brockmann, and T. Geisel. Forecast and control of epidemics in a globalized world. *Proceedings of the National Academy of Sciences*, 101(42):15124–15129,

October 2004.

- [10] P. H. Kao and R. J. Yang. Virus diffusion in isolation rooms. *Journal of Hospital Infection*, 62(3):338–345, March 2006.
- [11] Warren John Ewens. *Mathematical Population Genetics, I. Theoretical Introduction*, volume 27. 2012.
- [12] Ralf Metzler, Gleb Oshanin, and Sidney Redner. *First-Passage Phenomena and Their Applications*. World Scientific Publishing Co., January 2014.
- [13] David Waxman. The diffusion equation of random genetic drift—biology’s analogue of the Schrödinger equation? *Contemporary Physics*, 58(3):253–261, July 2017.
- [14] A. Einstein. über die von der molekularkinetischen Theorie der Wärme geforderte Bewegung von in ruhenden Flüssigkeiten suspendierten Teilchen. *Annalen der Physik*, 322(8):549–560, 1905.
- [15] A. Einstein. Zur Theorie der Brownschen Bewegung. *Annalen der Physik*, 324(2):371–381, 1906.
- [16] A. Einstein. Theoretische Bemerkungen Über die Brownsche Bewegung. *Zeitschrift für Elektrochemie und angewandte physikalische Chemie*, 13(6):41–42, 1907.
- [17] Firas Rassoul-Agha, Timo Seppäläinen, and Atilla Yilmaz. Quenched Free Energy and Large Deviations for Random Walks in Random Potentials. *Communications on Pure and Applied Mathematics*, 66(2):202–244, 2013.
- [18] Robert Brown. XXVII. A brief account of microscopical observations made in the months of June, July and August 1827, on the particles contained in the pollen of plants; and on the general existence of active molecules in organic and inorganic bodies. *The Philosophical Magazine*, 4(21):161–173, September 1828.
- [19] Robert Brown. XXIV. Additional remarks on active molecules. *The Philosophical Magazine*, 6(33):161–166, September 1829.
- [20] Paul Langevin. Sur la theorie du mouvement brownien. *Compt. Rendus*, 146:530–533, 1908.
- [21] William Sutherland. LII. The viscosity of gases and molecular force. *The London, Edinburgh, and Dublin Philosophical Magazine and Journal of Science*, 36(223):507–531, December 1893.
- [22] William Sutherland. LXXV. A dynamical theory of diffusion for non-electrolytes and the molecular mass of albumin. *The London, Edinburgh, and Dublin Philosophical Magazine and Journal of Science*, 9(54):781–785, June 1905.
- [23] M. von Smoluchowski. Zur kinetischen Theorie der Brownschen Molekularbewegung und der Suspensionen. *Annalen der Physik*, 326(14):756–780, 1906.
- [24] M. Von Smoluchowski. Notiz uiber die Berechnung der Brownschen Molekularbewegung bei der Ehrenhaft-Millikanschen Versuchsanordnung. *Phys. Z*, 16:318–321, 1915.
- [25] Jean Baptiste Perrin. Le Mouvement Brownien et la Réalité Moleculaire. *Ann. Chim. Phys.*, 18(8):5–114, 1909.
- [26] Jean Perrin. Mouvement brownien et molécules. *Journal de Chimie Physique*, 8:57–91, 1910.
- [27] G. E. Uhlenbeck and L. S. Ornstein. On the Theory of the Brownian Motion. *Physical Review*, 36(5):823–841, September 1930.
- [28] Andrew P. Hammond and Eric I. Corwin. Direct measurement of the ballistic motion of a freely floating colloid in Newtonian and viscoelastic fluids. *Physical Review E*, 96(4):042606–042606, October 2017.
- [29] Bo Wang, James Kuo, Sung Chul Bae, and Steve Granick. When Brownian diffusion is not Gaussian. *Nature Materials*, 11(6):481–485, May 2012.
- [30] Jean Philippe Bouchaud and Antoine Georges. Anomalous diffusion in disordered media: Statistical mechanisms, models and physical applications. *Physics Reports*, 195(4-5):127–293, November 1990.
- [31] Ralf Metzler. Brownian motion and beyond: First-passage, power spectrum, non-Gaussianity, and anomalous diffusion. *Journal of Statistical Mechanics: Theory and Experiment*, 2019(11):114003–114003, November 2019.
- [32] Sriram Ramaswamy. The Mechanics and Statistics of Active Matter. *Annual Review of Condensed Matter Physics*, 1(1):323–345, 2010.
- [33] Kiyoshi Kanazawa, Tomohiko G. Sano, Andrea Cairoli, and Adrian Baule. Loopy Lévy flights enhance tracer diffusion in active suspensions. *Nature*, 579(7799):364–367, March 2020.
- [34] Ronen Zangi and Laura J. Kaufman. Frequency-dependent Stokes-Einstein relation in supercooled liquids. *Physical Review E*, 75(5):051501, May 2007.
- [35] A. A. Chernov. Replication of a multicomponent chain by the “lightning” mechanism. *Biophysics*, 12(2), 1967.
- [36] D. E. Temkin. One-dimensional random walks in a two-component chain. *Soviet Math. Docl.*, 13:1172–1176, 1972.
- [37] Shlomo Havlin and Daniel Ben-Avraham. Diffusion in disordered media. *Advances in Physics*, 36(6):695–798, January 1987.
- [38] Erwin Bolthausen and Alain-Sol Sznitman. *Ten Lectures on Random Media*. Birkhäuser Basel, 2002.
- [39] A.-S. Sznitman. Topics in random walks in random environment. Technical Report 92-95003-25-X, International Atomic Energy Agency (IAEA), 2004.
- [40] Zeitouni Ofer. Random walks in random environment. In *Lectures on Probability Theory and Statistics, Lecture Notes*, volume 1837 of *Math*, pages 189–312. Springer, Berlin, 2004.
- [41] H. Kesten, M. V. Kozlov, and F. Spitzer. A limit law for random walk in a random environment. *Compositio Mathematica*, 30(2):145–168, 1975.
- [42] Ya. G. Sinai. The Limiting Behavior of a One-Dimensional Random Walk in a Random Medium. *Theory of Probability & Its Applications*, 27(2):256–268, January 1983.
- [43] J. P Bouchaud, A Comtet, A Georges, and P Le Doussal. Classical diffusion of a particle in a one-dimensional random force field. *Annals of Physics*, 201(2):285–341, August 1990.
- [44] S. F. Burlatsky and John M. Deutch. Transient relaxation of a charged polymer chain subject to an external field in a random tube. *The Journal of Chemical Physics*, 109(6):2572–2578, August 1998.
- [45] Pierre Le Doussal, Cécile Monthus, and Daniel S. Fisher. Random walkers in one-dimensional random environments: Exact renormalization group analysis. *Physical Review E*, 59(5):4795–4840, May 1999.
- [46] Lewis Fry Richardson and Gilbert Thomas Walker. Atmospheric diffusion shown on a distance-neighbour graph. *Proceedings of the Royal Society of London. Series A, Containing Papers of a Mathematical and Physical Character*, 110(756):709–737, April 1926.

- [47] H. G. E. Hentschel and Itamar Procaccia. Relative diffusion in turbulent media: The fractal dimension of clouds. *Physical Review A*, 29(3):1461–1470, March 1984.
- [48] J. P. Bouchaud. Diffusion and Localization of Waves in a Time-Varying Random Environment. *Europhysics Letters (EPL)*, 11(6):505–510, March 1990.
- [49] M. Chertkov and G. Falkovich. Anomalous Scaling Exponents of a White-Advection Passive Scalar. *Physical Review Letters*, 76(15):2706–2709, April 1996.
- [50] Denis Bernard, Krzysztof Gawędzki, and Antti Kupiainen. Anomalous Scaling in the N-Point Functions of Passive Scalar. *Physical Review E*, 54(3):2564–2572, September 1996.
- [51] Marie-Caroline Jullien, Jérôme Paret, and Patrick Tabeling. Richardson Pair Dispersion in Two-Dimensional Turbulence. *Physical Review Letters*, 82(14):2872–2875, April 1999.
- [52] E. Balkovsky, G. Falkovich, and A. Fouxon. Intermittent Distribution of Inertial Particles in Turbulent Flows. *Physical Review Letters*, 86(13):2790–2793, March 2001.
- [53] F. Rassoul-Agha and T. Seppäläinen. An almost sure invariance principle for random walks in a space-time random environment. *Probability Theory and Related Fields*, 133(3):299–314, November 2005.
- [54] Jean-Dominique Deuschel, Xiaoqin Guo, and Alejandro F. Ramirez. Quenched invariance principle for random walk in time-dependent balanced random environment. *arXiv:1503.01964 [math]*, September 2016.
- [55] Marton Balazs, Firas Rassoul-Agha, and Timo Seppäläinen. The random average process and random walk in a space-time random environment in one dimension. *Communications in Mathematical Physics*, 266(2):499–545, September 2006.
- [56] Guillaume Barraquand and Ivan Corwin. Random-walk in Beta-distributed random environment. *Probability Theory and Related Fields*, 167(3-4):1057–1116, April 2017.
- [57] Ivan Corwin. The Kardar–Parisi–Zhang equation and universality class. *Random Matrices: Theory and Applications*, 01(01):1130001, January 2012.
- [58] Jeremy Quastel and Herbert Spohn. The One-Dimensional KPZ Equation and Its Universality Class. *Journal of Statistical Physics*, 160(4):965–984, August 2015.
- [59] Craig A. Tracy and Harold Widom. Level-spacing distributions and the Airy kernel. *Physics Letters B*, 305(1):115–118, May 1993.
- [60] Pierre Le Doussal and Thimothée Thiery. Diffusion in time-dependent random media and the Kardar-Parisi-Zhang equation. *Physical Review E*, 96(1):010102–010102, July 2017.
- [61] Guillaume Barraquand and Pierre Le Doussal. Moderate deviations for diffusion in time dependent random media. *Journal of Physics A: Mathematical and Theoretical*, 53(21):215002, May 2020.
- [62] Mehran Kardar, Giorgio Parisi, and Yi-Cheng Zhang. Dynamic Scaling of Growing Interfaces. *Physical Review Letters*, 56(9):889–892, March 1986.
- [63] Tomohiro Sasamoto and Herbert Spohn. One-Dimensional Kardar-Parisi-Zhang Equation: An Exact Solution and its Universality. *Physical Review Letters*, 104(23):230602, June 2010.
- [64] P. Calabrese, P. Le Doussal, and A. Rosso. Free-energy distribution of the directed polymer at high temperature. *EPL (Europhysics Letters)*, 90(2):20002, April 2010.
- [65] V. Dotsenko. Bethe ansatz derivation of the Tracy-Widom distribution for one-dimensional directed polymers. *EPL (Europhysics Letters)*, 90(2):20003, April 2010.
- [66] Gideon Amir, Ivan Corwin, and Jeremy Quastel. Probability Distribution of the Free Energy of the Continuum Directed Random Polymer in 1+1 dimensions. *Communications on Pure and Applied Mathematics*, 64(4):466–537, April 2011.
- [67] Christophe Sabot and Laurent Tournier. Random walks in Dirichlet environment: An overview. *Annales de la Faculté des sciences de Toulouse : Mathématiques*, 26(2):463–509, 2017.
- [68] Márton Balázs, Firas Rassoul-Agha, and Timo Seppäläinen. Large deviations and wandering exponent for random walk in a dynamic beta environment. *The Annals of Probability*, 47(4):2186–2229, July 2019.
- [69] Guillaume Barraquand and Mark Rychkovsky. Large deviations for sticky Brownian motions. *Electronic Journal of Probability*, 25(none):1–52, January 2020.
- [70] Dom Brockington and Jon Warren. The Bethe Ansatz for Sticky Brownian Motions. *arXiv:2104.06482 [math]*, April 2021.
- [71] Giancarlo Oviedo, Gonzalo Panizo, and Alejandro F. Ramirez. Second order fluctuations of large deviations for perturbed random walks. *arXiv:2108.02877 [math]*, August 2021.
- [72] Sergei Korotkikh. Hidden diagonal integrability of q-Hahn vertex model and Beta polymer model. *Probability Theory and Related Fields*, March 2022.
- [73] Alexandre Krajenbrink and Pierre Le Doussal. The crossover from the Macroscopic Fluctuation Theory to the Kardar-Parisi-Zhang equation controls the large deviations beyond Einstein’s diffusion. *arXiv:2204.04720 [cond-mat, physics:math-ph, physics:nlin]*, April 2022.
- [74] Tom Alberts, Kostya Khanin, and Jeremy Quastel. Intermediate Disorder Regime for Directed Polymers in Dimension 1+1. *Physical Review Letters*, 105(9):090603, August 2010.
- [75] Timothy Halpin-Healy and Kazumasa A. Takeuchi. A KPZ Cocktail-Shaken, not Stirred... *Journal of Statistical Physics*, 160(4):794–814, August 2015.
- [76] Ivan Corwin and Yu Gu. Kardar–Parisi–Zhang Equation and Large Deviations for Random Walks in Weak Random Environments. *Journal of Statistical Physics*, 166(1):150–168, January 2017.
- [77] William Feller. Diffusion Processes in Genetics. *Proceedings of the Second Berkeley Symposium on Mathematical Statistics and Probability*, 2:227–247, January 1951.
- [78] P. a. P. Moran. Random processes in genetics. *Mathematical Proceedings of the Cambridge Philosophical Society*, 54(1):60–71, January 1958.
- [79] W. G. Pollard and R. D. Present. On Gaseous Self-Diffusion in Long Capillary Tubes. *Physical Review*, 73(7):762–774, April 1948.
- [80] Sheida Ahmadi and Richard K. Bowles. Diffusion in quasi-one-dimensional channels: A small system n, p, T, transition state theory for hopping times. *The Journal of Chemical Physics*, 146(15):154505, April 2017.
- [81] See Supplemental Material at XXXX.
- [82] Michael Prähofer and Herbert Spohn. Universal Distributions for Growth Processes in 1+1 Dimensions and Random Matrices. *Physical Review Letters*, 84(21):4882–

4885, May 2000.

- [83] Sylvain Prolhac and Herbert Spohn. The height distribution of the KPZ equation with sharp wedge initial condition: Numerical evaluations. *Physical Review E*, 84(1):011119, July 2011.



## Supplemental Material

### I. NUMERICAL METHODS

We expand upon our description of the numerical methods used in our simulations. We consider varying system sizes from  $N = 10^2$  to  $N = 10^{300}$  with time varying from  $t = 0$  to  $t = 5000 \log(N)$ . We simulate such large systems by utilizing the full range of quadruple-precision floating point numbers and making approximations to the binomial distribution when dealing with sizes beyond our precision limits. In particular, for a site  $x$  at time  $t$  where the number of particles,  $N(x, t)$ , is below  $2^{31}$  we use the C++ Boost integer implementation of a binomial distributed random number generator to choose the number of particles that will move right versus left. Above  $2^{31}$  the integer implementation overflows and we instead approximate the binomial distribution by a Gaussian distribution of mean  $N(x, t)B(x, t)$  and variance  $N(x, t)B(x, t)(1 - B(x, t))$ , as dictated by the central limit theorem. For sufficiently large  $N(x, t)$ , the variance itself will fall outside of the precision of a quadruple floating point number. This occurs when  $N(x, t) > 10^{64}$ , above which we approximate the binomial simply by its mean. The number of particles that move right is then  $N(x, t)B(x, t)$ . These approximations are necessary given the limitations of our precision and do not seem to affect the behavior of the system in any significant manner.

When estimating the statistics (e.g. mean and variance) for  $\text{Max}_t^N$ ,  $\text{Env}_t^N$  and  $\text{Sam}_t^N$ , the optimal manner would be that for each  $N$  and  $t$  we simulate a large number of environments and then build up histograms for the behavior of these quantities with one data point corresponding to one environment. Of course, in numerically computing the quantities for time  $t$ , we naturally compute them for all times smaller than  $t$  too, but for the same environment. Moreover,  $\text{Env}_t^N$  can be computed simultaneously for all  $N$  and  $t$  relative to the same environment, providing even further computational savings. We employ this computationally efficient approach to couple together the estimation for different values of  $N$  and  $t$  to the same pool of environments. There is a cost, however, to doing this. For example, the statistics that we numerically compute for  $\text{Max}_t^N$  for time  $t$  and time  $t'$  will themselves be correlated since they are derived from studying the same collection of environments. This correlation seems to be short-lived in time though, and is only evident upon zooming into the numerical measurements, for instances as in the inset in Fig. 3 of the main text.

### II. ASYMPTOTIC THEORY RESULTS

#### A. SSRW $\text{Max}_t^N$

Assume that the ratio  $\hat{t} = t/\log(N)$  tends to some finite value. As explained in the main article, if  $\hat{t} < (\log(2))^{-1}$  then  $N \gg 2^t$ . In that case,  $p(t, t) = 2^{-t} \gg 1/N$  which means that it is highly likely that there are many particles occupying the right-most site at  $x = t$ . This implies that  $\text{Mean}(\text{Max}_t^N) \approx t$  and  $\text{Var}(\text{Max}_t^N) \approx 0$ .

When  $\hat{t} > (\log(2))^{-1}$ , the maximal random walk at time  $t$  will likely occur significantly below  $t$  and have non-trivial fluctuations which we now describe. For the SSRW, observe that  $p(2k - t, t) = 2^{-t} \binom{t}{k}$  for  $k = 0, \dots, t$ . Thus, using Stirling's formula for binomial coefficients (or more generally using Cramer's theorem from the large deviation theory for sums of independent identically distributed random variables) we arrive at the asymptotic for  $v \in (0, 1)$  that

$$P(vt, t) \approx e^{-tI_{\text{SSRW}}(v)} \quad \text{where} \quad I_{\text{SSRW}}(v) = \frac{1}{2}((1+v)\log(1+v) + (1-v)\log(1-v)). \quad (8)$$

$I_{\text{SSRW}}(v)$  is known of as the large deviation rate function for the SSRW.

We may now combine this with Eq. (2) of the main text to show that  $\text{Max}_t^N$  is approximately distributed as a Gumbel random variable with location  $\mu \approx t\hat{v}$  and shape  $\beta = 1/I'_{\text{SSRW}}(\hat{v})$ , where  $\hat{v} = I_{\text{SSRW}}^{-1}(1/\hat{t})$  (here  $f^{-1}$  means the inverse function and not the reciprocal). A Gumbel random variable with location  $\mu$  and shape  $\beta$  has

$$\text{cumulative distribution function } e^{-e^{-(x-\mu)/\beta}}, \quad \text{mean } \mu + \beta\gamma, \quad \text{and variance } \frac{\pi^2}{6}\beta^2, \quad (9)$$

where  $\gamma \sim .57721$  is the Euler-Mascheroni constant.

To see the above limit, observe that

$$\begin{aligned} \text{Prob}(\text{Max}_t^N \leq t\hat{v} + x) &= (1 - P_{\mathbf{B}}(t\hat{v} + x, t))^N \approx (1 - e^{-tI_{\text{SSRW}}(\hat{v} + x/t)})^N \\ &\approx (1 - e^{-tI_{\text{SSRW}}(\hat{v}) - I'_{\text{SSRW}}(\hat{v})x})^N = (1 - N^{-1}e^{-I'_{\text{SSRW}}(\hat{v})x})^N \approx e^{-e^{-I'_{\text{SSRW}}(\hat{v})x}}. \end{aligned}$$

The first equality follows from Eq. (2) of the main text, the second approximation uses (8), the third uses Taylor expansion, the fourth follows from the definition of  $\hat{v} = I_{\text{SSRW}}^{-1}(1/\hat{t})$ , while the final one uses the approximation  $(1 - x/N)^N \approx e^{-x}$ . Notice that in Taylor expanding we have assumed that lower order terms do not cause issues. This can be easily justified by going to further orders in the Stirling formula expansion.

Based on the above Gumbel asymptotics, we can now record the asymptotic form of the mean and variance of  $\text{Max}_t^N$  for the SSRW. Writing  $\hat{v}(\hat{t})$  to make this dependence explicit and recalling that  $\hat{t} = t/\log(N)$  we see that

$$\text{Mean}(\text{Max}_t^N) \approx t\hat{v}\left(\frac{t}{\log(N)}\right) + \frac{\gamma}{I'_{\text{SSRW}}\left(\hat{v}\left(\frac{t}{\log(N)}\right)\right)}, \quad \text{Var}(\text{Max}_t^N) \approx \frac{\pi^2}{6\left(I'_{\text{SSRW}}\left(\hat{v}\left(\frac{t}{\log(N)}\right)\right)\right)^2}. \quad (10)$$

Inverting  $I_{\text{SSRW}}$  to find  $\hat{v}(\hat{t})$  is non-trivial though can be done numerically or in certain limits. For instance, noting that for  $v$  near zero,  $I_{\text{SSRW}} \approx v^2/2$  we see that for  $\hat{t}$  near infinity,  $\hat{v}(\hat{t}) \approx \sqrt{2/\hat{t}}$  and hence  $I'_{\text{SSRW}}(\hat{v}(\hat{t})) \approx \sqrt{2/\hat{t}}$ . From this and (10) it follows that for  $\hat{t} \gg (\log(2))^{-1}$ , asymptotically

$$\text{Mean}(\text{Max}_t^N) \approx \left(\sqrt{2\log(N)} + \frac{\gamma}{\sqrt{2\log(N)}}\right)t^{1/2}, \quad \text{Var}(\text{Max}_t^N) \approx \frac{\pi^2}{12} \frac{t}{\log(N)}.$$

On the other hand, (10) also shows that as  $\hat{t}$  tends to  $(\log(2))^{-1}$  from above, the mean goes to  $t$  and the variance goes to zero.

## B. RWRE $\text{Env}_t^N$

Assume that the ratio  $\hat{t} = t/\log(N)$  tends to some finite value exceeding 1. The key theoretic result we use here is due to [56]. They show that for  $v \in (0, 1)$ ,

$$\log(P_{\mathbf{B}}(vt, t)) = -tI(v) + t^{1/3}\sigma(v)\chi_t \quad \text{where} \quad I(v) = 1 - \sqrt{1 - v^2}, \quad \sigma(v) = \left(\frac{2I(v)^2}{1 - I(v)}\right)^{1/3}. \quad (11)$$

Here  $I(v)$  is the large deviation rate function and  $\sigma(v)t^{1/3}$  is the scalings of the random environment-dependent fluctuations  $\chi_t$  around that rate function. [56] showed that as  $t \rightarrow \infty$ , the distribution of  $\chi_t$  converges to a Tracy-Widom GUE distribution  $\chi$ . For reference below, let us note that [82]

$$\mu_\chi := \text{Mean}(\chi) \approx -1.771, \quad \sigma_\chi^2 := \text{Var}(\chi) \approx .813.$$

As in the case of the SSRW, we now solve for  $\hat{v} = \hat{v}(\hat{t})$  such that  $P_{\mathbf{B}}(\hat{v}t, t) = 1/N$ . Note that  $\hat{v}t$  will then equal the  $1/N$ -quantile  $\text{Env}_t^N$ . From (11),  $\hat{v}$  must satisfy

$$tI(\hat{v}) - t^{1/3}\sigma(\hat{v})\chi_t = \log(N) = t/\hat{t}. \quad (12)$$

Canceling  $t$  and dropping the  $t^{1/3}$  term momentarily yields to first order that  $\hat{v}$  is given by

$$\hat{v}_0 = I^{-1}(1/\hat{t}) = \sqrt{1 - (1 - 1/\hat{t})^2}.$$

We can now Taylor expand  $I(\hat{v})$  and  $\sigma(\hat{v})$  in (12) around  $\hat{v} = \hat{v}_0$  and solve for  $\hat{v}$  to the next order. Doing so we find that

$$\hat{v} = \hat{v}_0 + t^{-2/3} \frac{\sigma(\hat{v}_0)}{I'(\hat{v}_0)} \chi_t + O(t^{-4/3}).$$

Recalling that  $\hat{v}t$  is supposed to yield the  $1/N$ -quantile, we conclude that

$$\text{Env}_t^N = \hat{v}_0 t + t^{1/3} \frac{\sigma(\hat{v}_0)}{I'(\hat{v}_0)} \chi_t + O(t^{-1/3}). \quad (13)$$

From this we can extract the asymptotic mean and variance of  $\text{Env}_t^N$ . Written explicitly (i.e., plugging in  $I$  and  $\hat{v}_0$ ) this yields the following asymptotic formulas

$$\begin{aligned} \text{Mean}(\text{Env}_t^N) &\approx M_1(N, t) := \left(1 - \left(1 - \frac{\log(N)}{t}\right)^2\right)^{1/2} t + (\log(N))^{2/3} t^{-1/3} \frac{2^{1/3} \left(1 - \frac{\log(N)}{t}\right)^{2/3}}{\sqrt{1 - \left(1 - \frac{\log(N)}{t}\right)^2}} \mu_\chi \\ \text{Var}(\text{Env}_t^N) &\approx V_1(N, t) := \left(\frac{\log(N)}{t}\right)^{2/3} \frac{2^{2/3} \left(1 - \frac{\log(N)}{t}\right)^{4/3}}{1 - \left(1 - \frac{\log(N)}{t}\right)^2} \sigma_\chi^2, \end{aligned}$$

where above we have used that

$$\frac{\sigma(\hat{v}_0)}{I'(\hat{v}_0)} = \frac{2^{1/3} \hat{t}^{-2/3} (1 - 1/\hat{t})^{2/3}}{\sqrt{1 - (1 - 1/\hat{t})^2}}.$$

For  $\hat{t} = t/\log(N)$  large, it follows from the above expressions that

$$\text{Var}(\text{Env}_t^N) \approx \sigma_\chi^2 \left(\frac{\log(N)}{2}\right)^{\frac{1}{3}} t^{\frac{1}{3}}. \quad (14)$$

It is important to understand the order of the limits here. First we should fix  $\hat{t} = t/\log(N)$  and take  $N$  and  $t$  to infinity. Then we take  $\hat{t}$  large and find the above 1/3 power-law. That said, with some additional work using the methods of [56] it is possible to show that for the entire range  $1 \ll t/\log(N) \ll \log(N)$ , this 1/3 power-law persists. We will not provide the details for that here. However, below we will consider when  $t$  is of order  $(\log(N))^2$ . In that case, for small  $t$  in that range, we will find a perfect fit to the 1/3 power-law, thus agreeing with the assertion that this power-law persists over the full range  $1 \ll t/\log(N) \ll \log(N)$ .

Now assume that the ratio  $\hat{t} = t/\log(N)^2$  remains strictly positive and finite as  $N$  and  $t$  tend to infinity. While [56] probes  $P_{\mathbf{B}}(x, t)$  for  $x$  linearly growing with  $t$ , [61] probes the regime where  $x$  grows like  $t^{3/4}$ . They show that for  $v \in (0, \infty)$ ,

$$\log(P_{\mathbf{B}}(vt^{3/4}, t)) \approx -\frac{v^2 t^{1/2}}{2} - \frac{\log(t)}{4} + \log(v) - \frac{v^4}{12} + h(0, v^4) \quad (15)$$

where  $h(y, s)$  denotes the (random) height at spatial position  $y$  and time  $s$  of the *narrow wedge solution to the Kardar-Parisi-Zhang (KPZ) equation*

$$\partial_s h(y, s) = \frac{1}{2} \partial_y^2 h(y, s) + \frac{1}{2} (\partial_y h(y, s))^2 + \xi(y, s)$$

driven by space-time white noise  $\xi$ , see [57, 62]. Using this result, we will be able to prove this other  $(\log(N))^2$  time scale.

We may solve (15) perturbatively (as in the  $\log(N)$  case) for  $\hat{v}$  such that  $P_{\mathbf{B}}(\hat{v}t^{3/4}, t) = 1/N$ . The  $1/N$ -quantile  $\text{Env}_t^N = \hat{v}t^{3/4}$  is then given by

$$\text{Env}_t^N \approx \hat{v}_0 t^{3/4} + \frac{t^{1/4}}{\hat{v}_0} \left( h(0, \hat{v}_0^4) - \frac{\hat{v}_0^4}{12} - \log(\hat{v}_0) \right) + O(t^{-1/4}) \quad \text{where} \quad \hat{v}_0 = 2^{1/2} \hat{t}^{-1/4}.$$

From this we can explicitly compute the asymptotics of the mean and variance as

$$\begin{aligned} \text{Mean}(\text{Env}_t^N) &\approx M_2(N, t) := (2t \log(N))^{1/2} + \sqrt{\frac{t}{2 \log(N)}} \text{Mean} \left( h \left( 0, \frac{4(\log(N))^2}{t} \right) \right) \\ \text{Var}(\text{Env}_t^N) &\approx V_2(N, t) := \frac{t}{2 \log(N)} \cdot \text{Var} \left( h \left( 0, \frac{4(\log(N))^2}{t} \right) \right). \end{aligned} \quad (16)$$

Notice that in the mean we have dropped the lower order contributions from the terms  $\frac{\hat{v}_0^4}{12}$  and  $\log(\hat{v}_0)$ . The values of  $\text{Mean}(h(0, s))$  and  $\text{Var}(h(0, s))$  for varying  $s > 0$  can be computed numerically through evaluation of the Fredholm determinant formula from [63–66]. The result of this computation is recorded as Fig. 3 of [83]. In particular, the horizontal axis (labeled  $t$  in [83]) corresponds to our  $s$  variable, and the red circles record the value of  $\text{Mean} \left( \frac{h(0, s) + \frac{s}{24}}{(s/2)^{1/3}} \right)$  while the blue triangles record the values of  $\text{Var} \left( \frac{h(0, s) + \frac{s}{24}}{(s/2)^{1/3}} \right)$  (note that the  $s/24$  shift here does not change the variance

as it is deterministic). For  $s > .33$  we approximate the mean and variances by interpolating between the numerically evaluated values in [83] (S. Prohac kindly provided the data set used to create Fig. 3 in that paper). For  $s < .33$  we use the short-time behavior of the KPZ equation explained below for our values of the mean and variance.

There are two key asymptotics for  $h(0, s)$  derived in [63–66]:  $\frac{h(0, s) + \frac{s}{24}}{(s/2)^{1/3}} \approx \chi$  as  $s \rightarrow \infty$  where  $\chi$  is a Tracy-Widom GUE distributed, and  $h(0, s) \approx -\frac{1}{2} \log(2\pi s) + s^{1/4} \pi^{1/4} 2^{-1/2} G$  as  $s \rightarrow 0$  where  $G$  is standard Gaussian distributed. These imply corresponding asymptotics for the mean and variance. In particular, as  $\hat{t} \rightarrow 0$ ,

$$\text{Var}(\text{Env}_t^N) \approx \sigma_\chi^2 2^{-1/3} \log(N) \hat{t}^{1/3} = \sigma_\chi^2 \left(\frac{\log(N)}{2}\right)^{\frac{1}{3}} t^{\frac{1}{3}}$$

which agrees perfectly with (14). This shows that the long-time behavior in the  $t = O(\log(N))$  scaling regime and the short time behavior in the  $t = O(\log(N)^2)$  scaling regime match even up to the pre-factor. This strongly suggests the  $1/3$  power-law in Eq. 5 of the main text for the entire regime  $1 \ll t/\log(N) \ll \log(N)$ .

On the other hand, from the short-time KPZ asymptotic we find that as  $\hat{t} \rightarrow \infty$ ,

$$\text{Var}(\text{Env}_t^N) \approx \frac{1}{2} \pi^{1/2} t^{1/2}$$

thereby recovering Eq. (5) for the regime  $t \gg (\log(N))^2$  in the main text. This indicates that for finite  $N$  and  $t$  it is necessary to stitch together the two regimes to get a reasonable formula for  $\text{Var}(\text{Env}_t^N)$ . We have found that an error function centered at  $t = (\log(N))^{3/2}$  with a width of  $(\log(N))^{4/3}$  produces a smooth transition between the two regimes. Thus, our final expression for the asymptotic mean and variance is given by

$$\text{Var}^{\text{asy}}(\text{Env}_t^N) = \frac{1 - \text{erf}\left(\frac{t - (\log(N))^{3/2}}{(\log(N))^{4/3}}\right)}{2} V_1(N, t) + \frac{1 + \text{erf}\left(\frac{t - (\log(N))^{3/2}}{(\log(N))^{4/3}}\right)}{2} V_2(N, t), \quad (17)$$

provided that  $t \geq \log(N)$  and 0 for  $t < \log(N)$ . Here  $\text{erf}(x) = 2/\sqrt{\pi} \int_0^x e^{-t^2} dt$  is the error function. This construction is shown in Fig. 6. On the other hand, such stitching is unnecessary when it comes to the mean since the large  $t$  behavior of  $M_1(N, t)$  matches the behavior of  $M_2(N, t)$  all the way as  $t \rightarrow \infty$ . This can be seen through direct asymptotics of the formulas and is illustrated in Fig. 5. On this account, we simply take

$$\text{Mean}^{\text{asy}}(\text{Env}_t^N) = M_1(N, t). \quad (18)$$

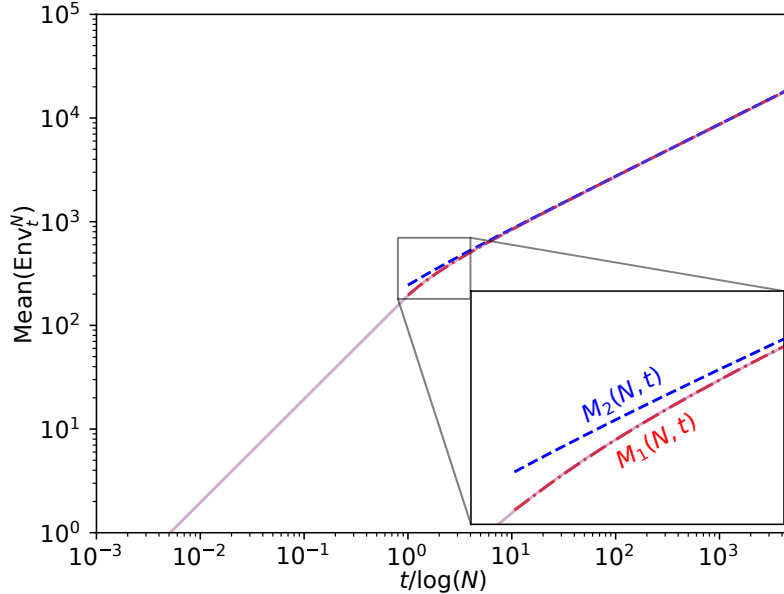


FIG. 5. The asymptotic mean functions  $M_1(N, t)$  and  $M_2(N, t)$  are plotted for  $N = 10^{85}$  in red and blue dashed lines, respectively. They agree closely for the full range of  $t > \log(N)$  and also match the numerically measured values  $\text{Mean}^{\text{num}}(\text{Max}_t^N)$  given by the purple curve (which is linear, as expected, until roughly time  $t = \log(N)$ ).

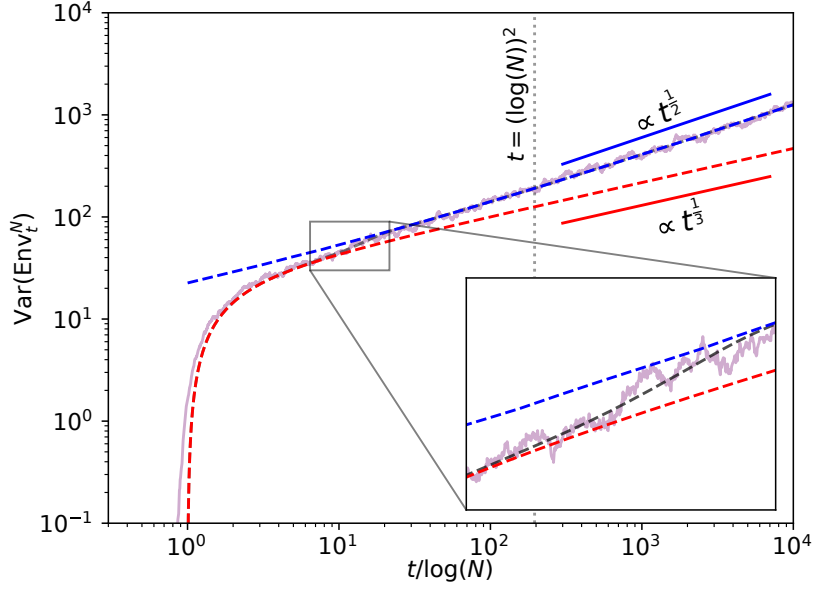


FIG. 6. The asymptotic variance functions  $V_1(N, t)$  and  $V_2(N, t)$  are plotted for  $N = 10^{85}$  in red and blue dashed lines, and the stitched together formula for  $\text{Var}^{\text{asy}}(\text{Env}_t^N)$  from (17) is plotted as the black dashed line. The purple curve is the numerically measured curve  $\text{Var}^{\text{num}}(\text{Env}_t^N)$ . The inset shows how the stitching captures the transition between the two asymptotic curves  $V_1$  and  $V_2$ , and the solid lines show the asymptotic power-laws that  $V_1$  and  $V_2$  demonstrate as  $t \rightarrow \infty$ . The vertical dotted line indicates the regime crossover at  $t = (\log(N))^2$ .

### C. RWRE $\text{Sam}_t^N$ and $\text{Max}_t^N$

Assume for the moment that  $t = \hat{t} \log(N)$  for  $\hat{t} > 1$ . Then (11) implies that

$$P_{\mathbf{B}}(\text{Env}_t^N + x, t) = \exp\left(-tI\left(\frac{\text{Env}_t^N}{t} + \frac{x}{t}\right) + t^{1/3}\sigma\left(\frac{\text{Env}_t^N}{t} + \frac{x}{t}\right)\chi_t\right) \quad \text{and} \quad P_{\mathbf{B}}(\text{Env}_t^N, t) = \frac{1}{N}.$$

If we Taylor expand to the next order in the exponential we find

$$\begin{aligned} P_{\mathbf{B}}(\text{Env}_t^N + x, t) &\approx \exp\left(-tI\left(\frac{\text{Env}_t^N}{t}\right) - I'\left(\frac{\text{Env}_t^N}{t}\right)x + t^{1/3}\sigma\left(\frac{\text{Env}_t^N}{t}\right)\chi_t\right) \\ &= \frac{1}{N}e^{-I'\left(\frac{\text{Env}_t^N}{t}\right)x} \approx \frac{1}{N}e^{-I'(\hat{v}(\hat{t}))x}. \end{aligned}$$

The Taylor expansion requires a bit of explanation. We expand  $I\left(\frac{\text{Env}_t^N}{t} + \frac{x}{t}\right) \approx I\left(\frac{\text{Env}_t^N}{t}\right) + I'\left(\frac{\text{Env}_t^N}{t}\right)\frac{x}{t}$  to first order. The similar expansion of  $\sigma$  would produce a lower order term. However, there is a subtlety that we should point out. The  $\chi_t$  random variable implicitly depends on  $x$  as well. Namely, if we look at the random transition probability as we vary around  $\text{Env}_t^N$ , the fluctuations of this quantity will vary with  $x$ . However, we assume here that this fluctuation does not contribute to leading order. We do not attempt to justify this theoretically here, though note that it yields very good agreement with our numerical simulations. The final approximation in the above string of equations involves replacing  $I'\left(\frac{\text{Env}_t^N}{t}\right)x$  by  $I'(\hat{v}(\hat{t}))x$  which relies on the fact that  $\frac{\text{Env}_t^N}{t} \approx \hat{v}_0$  to highest order.

Combining the above deduction with (2) in the main text and  $(1-x)^N \approx e^{-xN}$  (for  $x$  small) yields

$$\text{Prob}(\text{Max}_t^N \leq \text{Env}_t^N + x) \approx \left(1 - \frac{1}{N}e^{-I'(\hat{v}(\hat{t}))x}\right)^N \approx e^{-e^{-I'(\hat{v}(\hat{t}))x}}. \quad (19)$$

If we define  $\text{Sam}_t^N$  by the equality  $\text{Max}_t^N = \text{Env}_t^N + \text{Sam}_t^N$  then the above calculation shows that  $\text{Sam}_t^N$  is asymptotically independent of  $\text{Env}_t^N$  and asymptotically is Gumbel distributed with location and shape parameters

$$\mu(t) = 0, \quad \beta(t) = 1/I'(\hat{v}(\hat{t})) = (\hat{t} - 1)(2\hat{t} - 1)^{-1/2} \approx (\hat{t}/2)^{1/2}$$

where the approximation is for  $\hat{t} \gg 1$ . This justifies the addition law for variances (Eq. (7) in the main text)

$$\text{Var}(\text{Max}_t^N) \approx \text{Var}(\text{Env}_t^N) + \text{Var}(\text{Sam}_t^N) \quad (20)$$

and (using the Gumbel variance formula in (9)) this also justifies Eq. (6) of the main text which provides the asymptotic formula for the variance (we also record that the asymptotic mean is 0)

$$\text{Mean}^{\text{asy}}(\text{Sam}_t^N) = 0, \quad \text{Var}^{\text{asy}}(\text{Sam}_t^N) = \frac{\pi^2}{6 \log(N)} \frac{\left(\frac{t}{\log(N)} - 1\right)^2}{2 \frac{t}{\log(N)} - 1} \approx \frac{\pi^2}{12 \log(N)} t, \quad (21)$$

where the approximation is for  $\hat{t} \gg 1$ .

Putting together (17), (18), (20) and (21) we conclude that

$$\begin{aligned} \text{Mean}^{\text{asy}}(\text{Max}_t^N) &= M_1(N, t), \\ \text{Var}^{\text{asy}}(\text{Max}_t^N) &= \frac{1 - \text{erf}\left(\frac{t - (\log(N))^{3/2}}{(\log(N))^{4/3}}\right)}{2} V_1(N, t) + \frac{1 + \text{erf}\left(\frac{t - (\log(N))^{3/2}}{(\log(N))^{4/3}}\right)}{2} V_2(N, t) \\ &\quad + \frac{\pi^2}{6 \log(N)} \frac{\left(\frac{t}{\log(N)} - 1\right)^2}{2 \frac{t}{\log(N)} - 1}. \end{aligned} \quad (22)$$

The above calculation assumed  $\hat{t} = t/\log(N)$  converges to a finite value. However, in a similar manner based on (15) we can probe the behavior when  $\hat{t} = t/(\log(N))^2$  converges to a finite value. This behavior agrees perfectly with the large  $\hat{t}$  limiting behavior above. Thus, we conclude that the formula for  $\text{Var}^{\text{asy}}(\text{Sam}_t^N)$  should hold for all  $t \gg \log(N)$ .

Fig. 7 and Fig. 8 show our asymptotic theory formulas for the mean of the maximal particle fit closely with our numerical simulations.

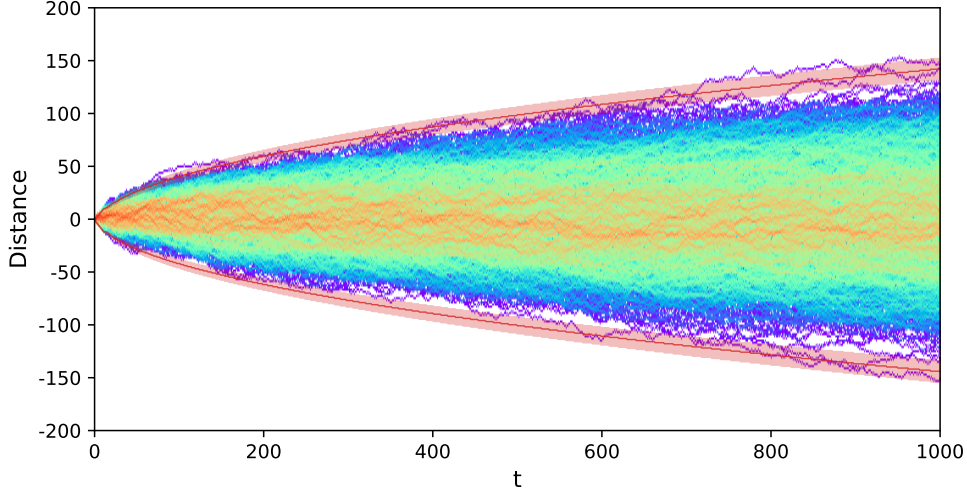


FIG. 7. A system of  $N = 10^5$  particles evolving in a given random environment. The heat map records the site occupancy density. We also plot in red  $\text{Mean}^{\text{asy}}(\text{Max}_t^N)$ , the asymptotic theory mean location for the maximum particle location given in Eq. (22). Around this is a pink shaded region of width  $2\sqrt{\text{Var}^{\text{asy}}(\text{Max}_t^N)}$ , i.e. given by one standard deviation based on the asymptotic theory variance formula also given in Eq. (22). This region generally contains the extreme-most particle over time.

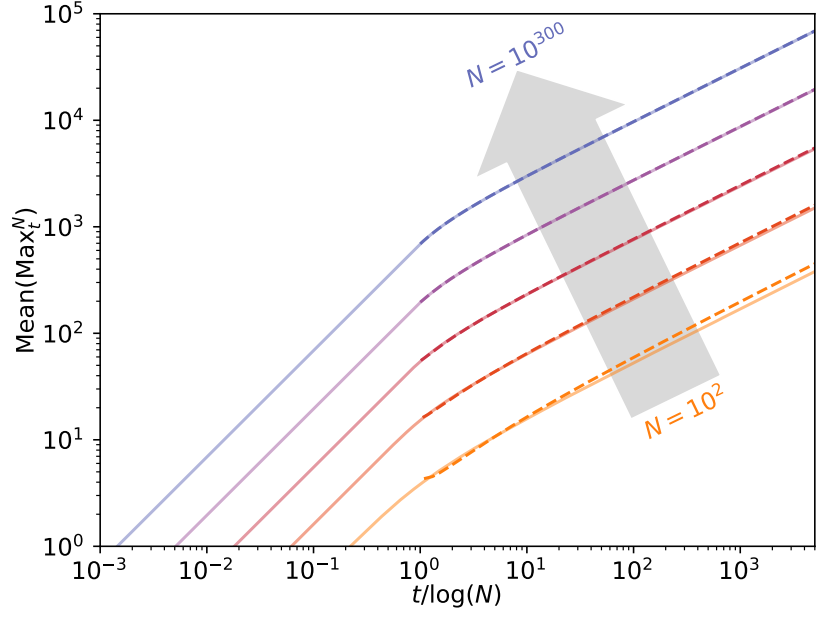


FIG. 8. The mean position of the maximal particle location (solid line) for  $N = 10^2, 10^7, 10^{24}, 10^{85}$  and  $10^{300}$  for 10000, 5000, 1500, 500 and 500 instantiations of the environment, respectively. The theoretical prediction (dashed line) given in Eq. (22) is also shown. We find the theoretical predictions for the mean position of the maximum particle,  $\text{Mean}(\text{Max}_t^N)$ , are in agreement with the data.